

Enhancement of Superconductivity in a Dirty Marginal Fermi Liquid

Tsz Chun Wu,¹ Patrick A. Lee,² and Matthew S. Foster^{1,3}

¹*Department of Physics and Astronomy, Rice University, Houston, Texas 77005, USA*

²*Department of Physics, Massachusetts Institute of Technology, Cambridge, Massachusetts 02139, USA*

³*Rice Center for Quantum Materials, Rice University, Houston, Texas 77005, USA*

(Dated: May 24, 2023)

We study superconductivity in a two-dimensional, disordered marginal Fermi liquid. At the semi-classical level, the transition temperature T_c is strongly suppressed because marginal Fermi liquid effects destroy well-defined quasiparticles. However, we show that interference between quantum-critical collective modes must be included, and these *enhance* T_c , violating Anderson's theorem. Our results suggest that phase coherence in a disordered, quantum-critical system can survive and manifest in the form of collective excitations, despite the absence of coherent quasiparticles.

The strange metal behavior has been a persistent mystery for over 30 years [1] and by now has been observed in a wide range of quantum materials including the cuprates [2] and twisted bilayer graphene [3]. Recent theoretical results suggest that quantum-critical interactions *and* disorder are both key ingredients for strange metallicity [4–7]. In particular, Refs. [8, 9] have proposed microscopic models based on the interplay between a critical mode and disorder that address aspects of the disordered marginal Fermi liquid (MFL) phenomenology. The next challenge is to understand the interplay of critical interactions and disorder on superconductivity [10–19]. In this Letter we address a fundamental paradox: Why does superconductivity, a macroscopic, coherent many-body quantum state, arise at anomalously high temperatures from a collision-dominated, seemingly incoherent strange metal?

We extend Ref. [9] to include pairing due to an attractive interaction W . The phenomenological parameter W can originate from phonons or from integrating out short-scale fluctuations of the critical mode. The main physics result of this paper is that the transition temperature T_c in a disordered MFL can be significantly boosted by quantum interference corrections, *despite the absence of well-defined quasiparticles*:

$$T_c \sim \begin{cases} g^2(\nu_0 W_{\text{eff}}) \mathcal{C} / \sigma_{\text{dc}}, & T_c \gtrsim T_*, \\ g^2(\nu_0 W_{\text{eff}})^2 / \sigma_{\text{dc}}, & T_c \ll T_*. \end{cases} \quad (1)$$

This should be contrasted to the Bardeen-Cooper-Schrieffer (BCS) result $T_c^{\text{BCS}} \propto e^{-1/(\nu_0 W)}$. In Eq. (1), g is the Yukawa coupling between fermions and quantum-relaxational (critical) bosons. σ_{dc} is the total dc conductivity of the non-superconducting MFL state in units of e^2/\hbar , ν_0 is the density of states (DoS) per channel, and W_{eff} is the effective BCS attractive interaction strength renormalized by MFL effects. The dimensionless constant \mathcal{C} is non-universal, depending upon the model parameters. While Ref. [9] focused on the regime where the bosons are characterized by a thermal mass, Eq. (1) also includes the low- T limit $T < T_*$, where T_* marks the

crossover to the regime dominated by dynamical screening [19]. We note that the model without W was found to show a conductivity that diverges at low T [9]. If W is generated from ultraviolet fluctuations in the boson mode, our results suggest that the low temperature state of this model may be a superconductor that owes its existence to the interplay between a critical mode and disorder. While our results have been obtained in a large- N type model to facilitate a controlled expansion, we believe the conclusion is more general. In fact, similar results were very recently obtained in Ref. [19] for superconductivity near a ferromagnetic quantum critical point.

The effects of disorder on superconductivity remains an active area of research [19–56]. Anderson's theorem dictates that s -wave superconductivity is immune to non-magnetic disorder as long as the normal state is a good metal [20, 21]. However, a seminal work by Maekawa and Fukuyama revealed that Coulomb interactions can suppress superconductivity at the quantum level, due to Anderson localization [22], enriching the original statement of the theorem. This scenario has been further investigated using field-theoretical methods [25, 27].

Interestingly, recent developments suggest a new twist of this theme: short-ranged (e.g., externally screened Coulomb) interactions and random or structural inhomogeneity can enhance superconductivity near the Anderson metal-insulator transition [19, 31–37, 39, 40, 57]. Owing to quantum interference, single-particle wavefunctions exhibit multifractality and strong state-to-state overlaps [58], resulting in larger interaction matrix elements that promote the pairing amplitude [31, 32].

Quantum interference effects like multifractality might be expected to play no role in a strongly correlated non-Fermi liquid lacking long-lived quasiparticles. An intensively studied paradigm for such systems consists of two-dimensional (2D) fermions at finite density coupled to quantum-critical bosons [7, 59–61]. Due to the large decay rate, the Landau quasiparticle paradigm breaks down in these theories.

In this Letter we show that Eq. (1) arises due to the persistence of multifractal enhancement for collective

modes in a dirty MFL. In a dirty quantum-critical system, impurities can dramatically modify the self-energies of the bosons and fermions, due to disorder smearing. At finite temperature T and at the quantum critical point, the (retarded) bosonic propagator acquires a quantum relaxational form [4, 8, 9, 60]

$$D_b^R(\omega, \mathbf{k}) = -\frac{1}{2}[k^2 - i\alpha\omega + m_b^2(T)]^{-1}, \quad (2)$$

which is quite generic. Here, ω and k are frequency and momentum, α is a constant, and $m_b^2 = \alpha_m T$ is the thermal mass. The latter generically arises due to symmetry-allowed quartic bosonic interactions [4, 8, 9, 62]. With disorder, the bosons behave diffusively, in contrast with the clean self-energy $\sim \omega/k$. Consequently, the fermionic self-energy acquires a MFL form for $T > T_*$ [1, 4, 8, 9]:

$$\begin{aligned} \Sigma_f^R(\omega) &= -i\gamma_{\text{el}} + \Sigma_{\text{MFL}}^R(\omega), \\ \Sigma_{\text{MFL}}^R(\omega) &= -\bar{g}^2 \left(\omega \ln \frac{\omega_c}{x} + i\frac{\pi}{2}x \right), \end{aligned} \quad (3)$$

in contrast with its clean counterpart that scales as $\sim |\omega|^{2/3}$. Here, $x = \max(|\omega|, JT)$, $\bar{g}^2 \sim g^2/\gamma_{\text{el}}$, g is the fermion-boson Yukawa coupling, J is a slowly varying dimensionless function of α/α_m [9], which we take to be a constant, ω_c is a cutoff, and γ_{el} is the self-consistent Born impurity scattering rate. The MFL self-energy indicates that the concept of quasiparticles is ill-defined due to the strong quantum-critical interaction. While this Planckian dissipation suppresses the phase coherence seemingly necessary for pairing [63], superconductivity has been observed in a wide range of quantum-critical systems. How can superconductivity survive when the single-particle phase coherence ceases to exist?

In this Letter, we show that not only does superconductivity survive in a disordered MFL, it can be enhanced owing to the interplay of the diffusive collective modes and quantum-relaxational bosons. We focus on the effects of Gaussian-distributed on-site impurity potential disorder and ignore randomness in the fermion-boson Yukawa coupling g [7, 18]. We elucidate the physics by carrying out an explicit calculation using the Finkelstein non-linear sigma model (FNLsM) [9, 64–68], which is a field-theoretical tool governing the interacting diffusive collective modes.

Evaluation of the Cooperon ladder diagram [24, 67] reveals that the finite-temperature pairing susceptibility is strongly suppressed due to the MFL self-energy in Eq. (3). This is however only the *semiclassical* approximation to the pairing susceptibility. We also compute the Maekawa-Fukuyama diagrams [22, 25] that describe quantum interference-mediated mixing of different interaction channels. The mixing of long-ranged Coulomb and BCS interactions is well-known to suppress superconductivity, and is a precursor to the superconductor-insulator transition [25, 40]. The mixing with short-

range or other interaction channels can boost superconductivity, attributed to the enhancement of matrix elements amongst critical (multifractal) wave functions [31–34, 37]. We will show that the quantum correction to the semiclassical result predicts robust superconductivity of non-BCS form, Eq. (1).

Model.—We consider a system with N flavors of fermions coupled to $SU(N)$ matrix bosons describing the collective modes tuned to the quantum critical point [9, 69, 70]. In the presence of disorder, the bosons become quantum relaxational and the fermions behave as in a dirty MFL [6, 8, 9]. We start with the FNLsM [9, 64–67] governing the diffusive collective modes within the Keldysh framework in class AI (orthogonal) [71, 72], in which spin-rotational and time-reversal symmetries are preserved. The FNLsM can be derived by following the standard procedures of disorder averaging, \hat{q} -matrix decoupling, and gradient expansion by assuming $v_F k, \omega \ll \gamma_{\text{el}}$ (v_F is the Fermi velocity). The corresponding partition function and action are given respectively by [9, 65]

$$Z = \int \mathcal{D}\hat{q} \mathcal{D}\hat{\phi} \mathcal{D}|\Delta|^2 e^{-S}, \quad (4)$$

$$S = S_q + S_\phi + S_{q\phi} + S_\Delta + S_{q\Delta}, \quad (5)$$

where

$$\begin{aligned} S_q &= \frac{\pi\nu_0 D}{8} \int_{\mathbf{x}} \text{Tr} [\nabla\hat{q} \cdot \nabla\hat{q}] \\ &\quad + \frac{i\pi\nu_0}{2} \int_{\mathbf{x}} \text{Tr} [\hat{q} \hat{\sigma}^3 (\hat{\omega} - \hat{\Sigma})], \end{aligned} \quad (6)$$

$$S_\phi = -\frac{i}{2} \int_{\omega, \mathbf{k}} \text{Tr} \left\{ \hat{\phi}_{-\omega, -\mathbf{k}}^T [\hat{D}_b(\omega, \mathbf{k})]^{-1} \hat{\phi}_{\omega, \mathbf{k}} \right\}, \quad (7)$$

$$S_{q\phi} = -i\pi\nu_0 \frac{g}{\sqrt{N}} \int_{\mathbf{x}} \text{Tr} [\hat{\Phi}(\mathbf{x}) \hat{q}(\mathbf{x})], \quad (8)$$

$$S_\Delta = -i\frac{2N}{W} \int_{t, \mathbf{x}} (\bar{\Delta}^q \Delta^{\text{cl}} + \Delta^q \bar{\Delta}^{\text{cl}}), \quad (9)$$

$$S_{q\Delta} = \frac{i\pi\nu_0}{2} \int_{\mathbf{x}} \text{Tr} [\hat{\hat{\Delta}}(\mathbf{x}) \hat{q}(\mathbf{x})]. \quad (10)$$

We adopted the shorthand notation $\int_{t, \mathbf{x}} = \int dt \int d^2x$ and $\int_{\omega, \mathbf{k}} = \int d\omega d^2k / (2\pi)^3$. The matrix field $\hat{q} \rightarrow \hat{q}_{\sigma, \sigma'; \alpha, \beta; i, j; \omega, \omega'}^{a, b}(\mathbf{x})$ incorporates both particle-hole (diffuson) and particle-particle (Cooperon) modes of the fermions, and carries particle-hole $\{\sigma, \sigma'\}$, spin-1/2 $\{\alpha, \beta\}$, $SU(N)$ flavor $\{i, j\}$, and Keldysh $\{a, b\}$ indices as well as frequency labels $\{\omega, \omega'\}$. It obeys the constraints $\text{Tr}[\hat{q}] = 0$, $\hat{q}^2 = 1$, and $\hat{s}^2 \hat{\sigma}^1 \hat{\tau}^1 \hat{\Theta}^1 \hat{q}^T \hat{s}^2 \hat{\sigma}^1 \hat{\tau}^1 \hat{\Theta}^1 = \hat{q}$. Pauli matrices $\hat{\sigma}$, \hat{s} , $\hat{\tau}$, and $\hat{\Theta}$ act respectively in the particle-hole, spin, Keldysh, and frequency spaces [65].

$D = v_F^2/4\gamma_{el}$ is the fermion diffusion constant. The quantum-relaxational boson is denoted $\hat{\phi}$; this is a matrix in flavor but a local field in space and time. Superconductivity arises via condensation of the local spin-singlet pairing fields $\{\hat{\Delta}, \Delta\}$; W denotes bare the BCS coupling.

The \hat{q} -matrix action differs from the Fermi-liquid case in the second line of Eq. (6), where it incorporates the MFL self-energy $\hat{\Sigma} \equiv \text{diag}\{\Sigma_{\text{MFL}}^R, \Sigma_{\text{MFL}}^A\}_\tau$ [Eq. (3)]. This results in an anomalous diffusion propagator [9, 73]. The Yukawa and pairing interactions between \hat{q} , $\hat{\phi}$, and Δ appear in $S_{q\phi}$ and $S_{q\Delta}$. The fields $\hat{\Phi} \sim \hat{\phi}$ and $\hat{\mathcal{D}} \sim \Delta + \Delta$ incorporate appropriate matrix factors and Keldysh labels cl, q, omitted here for brevity [73].

Technically we consider flavor “triplet” pairing, wherein the pairing field [75]

$$\Delta_{\alpha,\beta;i,j} = \Delta_0 s_{\alpha\beta}^2 \delta_{ij}. \quad (11)$$

$SU(N > 2)$ does not permit condensation of flavor-singlet fermion pairs. A natural generalization of our work allowing genuine flavor-singlet pairs would incorporate $SO(N)$ antiferromagnetic bosons, but this requires the further incorporation of (e.g., weakly broken) particle-hole symmetry [76, 77].

Our goal is to evaluate the retarded pairing susceptibility χ^R by integrating out the \hat{q} matrix and bosonic $\hat{\phi}$ fields to obtain an effective propagator for the Δ field. We proceed by parameterizing \hat{q} with coordinates [9, 65] and derive a set of Feynman rules. In addition to $S_{q\phi}$ and $S_{q\Delta}$, there is a Hikami box quartic interaction term appearing after the parameterization of S_q . Diagram conventions follow Refs. [9, 65], see Ref. [73] for details.

Results.—At the semiclassical level, the Cooperon ladder contribution to the pairing susceptibility [24, 67] is diagrammatically depicted in Fig. 1(b). The double-dotted-line blue rectangle represents the Cooperon propagator. The associated frequency flow is depicted by the arrows on the blue lines, while the momentum flow is indicated by a short black arrow between them. The purple dot represents the vertex of the \hat{q} - Δ coupling. The corresponding (retarded) inverse pairing susceptibility as $T \rightarrow T_c$ is

$$[\chi_{\text{semi}}^R]^{-1}(\Omega \rightarrow 0, \mathbf{q} \rightarrow 0) = -\frac{2N}{W} + 2\pi\nu_0 N \mathcal{S}(t_c) = 0, \quad (12)$$

where

$$\mathcal{S}(t) = \int_{-1/t}^{1/t} \frac{dy}{2\pi} \frac{\tanh(y)}{y \mathcal{A}_{\text{MFL}}(y) + i/(4t\gamma_{el}\tau_\varphi)}, \quad (13)$$

$$\mathcal{A}_{\text{MFL}}(y) = 1 + \bar{g}^2 \ln \left[\frac{\omega_c/T}{\max(J, 2|y|)} \right], \quad (14)$$

$t \equiv T/\gamma_{el}$ and $\tau_\varphi^{-1} \equiv \tau_{\text{MFL}}^{-1} + \tau_C^{-1}$ is the dephasing rate that in principle contains effects from both the MFL and the Cooperon self-energy [65, 78]. To make the physical

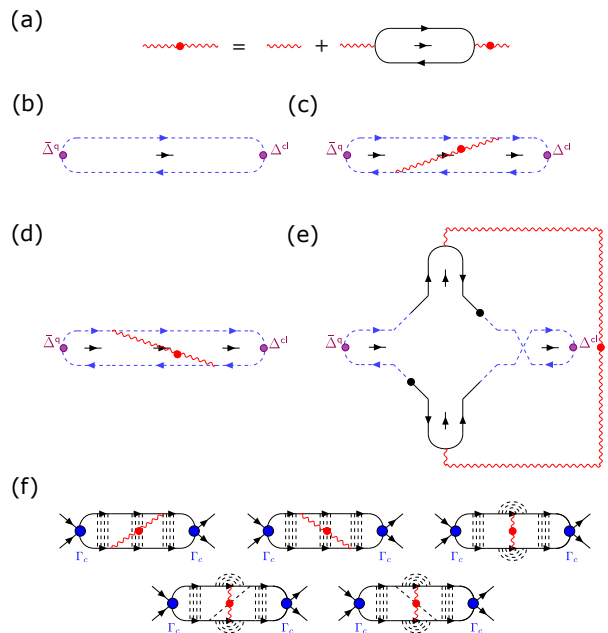


FIG. 1. (a): The Feynman diagram for the dynamically screened $SU(N)$ matrix boson propagator (red wavy line with a red dot) under the random phase approximation. The wavy line represents the quantum relaxational bosonic propagator D_b^R [Eq. (2)]. (b)–(e): The diagrams contributing to the inverse static pairing susceptibility $[\chi^R]^{-1}(\Omega = 0, \mathbf{q} = \mathbf{0})$: Panel (b) is the semiclassical Cooperon ladder contribution, see also Eq. (13). Panels (c)–(e) are the quantum interference corrections due to the interplay of diffusive collective modes (diffusons and Cooperons) and the attractive quantum-critical interaction, see Eq. (18). The diffuson propagator is represented diagrammatically by two black solid lines carrying counterpropagating arrows. Similarly, the Cooperon propagator is represented by two blue dashed lines. $\Delta^{cl/q}$ represents the Cooper pairing field. The vertex for the coupling between $\Delta^{cl/q}$ and the Cooperon is represented by the purple dot. More details appear in Ref. [73]. (f): The Feynman diagrams renormalizing the BCS channel scattering amplitude Γ_c in conventional many-body perturbation theory [22, 25]. These quantum corrections are analogous to diagrams (c)–(e) within the FNLsM. The dashed lines represent impurity scattering and solid black lines denote the fermionic Green’s functions.

picture more transparent, we will treat τ_C^{-1} as a phenomenological constant in this work for simplicity and defer a more detailed analysis to a separate study. The temperature dependence of \mathcal{S} for various \bar{g}^2 is shown in Fig. 2. At low temperatures, the dephasing rate drops out and \mathcal{S} can be estimated as

$$\mathcal{S}(t) \simeq \frac{1}{\pi \bar{g}^2} \ln(1 - \bar{g}^2 \ln t_c). \quad (15)$$

In the absence of the MFL self-energy ($\bar{g}^2 = 0$, black curve), \mathcal{S} diverges logarithmically as T decreases, resulting in the standard BCS result $T_c^{\text{BCS}} \propto e^{-1/\nu_0 W}$ for $1/T_c \tau_\varphi \ll 1$, independent of disorder and in accordance

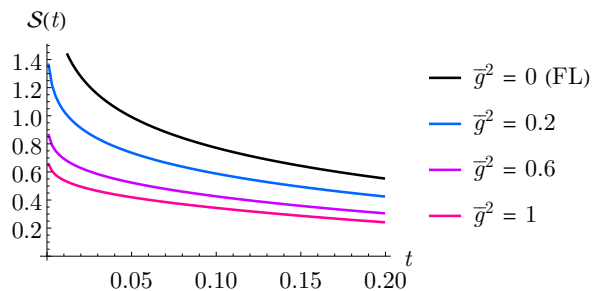


FIG. 2. Plot of the semiclassical Cooperon ladder integral $\mathcal{S}(T)$ in Eq. (13) as a function of the dimensionless temperature $t = T/\gamma_{\text{el}}$, for different reduced fermion-boson Yukawa couplings \bar{g}^2 (increasing from black to red). Here, the dephasing rate due to the Cooperon self-energy is chosen to be $\tau_C^{-1}/\gamma_{\text{el}} = 10^{-3}$. The black curve corresponds to the Fermi liquid case in which there is no marginal Fermi liquid (MFL) self-energy contribution. The singularity of \mathcal{S} is strongly suppressed by the MFL effects as \bar{g}^2 increases, owing to the absence of well-defined quasiparticles.

with Anderson's theorem. However, as \bar{g}^2 increases (blue to red), the logarithmic divergence is increasingly weakened by $\mathcal{A}_{\text{MFL}} > 1$, leading to a much smaller T_c . The suppression can be understood physically as a consequence of attempting to pair incoherent MFL fermions [63]. Although the MFL self-energy does *not* contribute to transport at the semiclassical level with a spatially uniform Yukawa coupling g [6, 8, 9], it strongly degrades superconductivity as there is no conservation law associated with the Cooperon propagator.

We now consider quantum interference corrections to the pairing susceptibility at the leading order of $1/\sigma_{\text{dc}}$. The corresponding Feynman diagrams are shown in Figs. 1(c)–(e). The double-line black rectangles denote diffuson propagator and the red wavy line represents the $\text{SU}(N)$ matrix boson. The red dot on the wavy line indicates that the bosonic propagator is dynamically screened, Fig. 1(a). At low temperatures, the retarded component of the dynamically screened bosonic propagator under the random phase approximation is

$$D_{\text{scr}}^R(\omega, \mathbf{k}) = \frac{1}{[D_{\text{b}}^R]^{-1}(\omega, \mathbf{k}) - \Pi_{\text{b}}^R(\omega, \mathbf{k})}, \quad (16)$$

$$\Pi_{\text{b}}^R(\omega, \mathbf{k}) \simeq \frac{2i}{N} \frac{\nu_0 g^2 \omega}{Dk^2 - i\omega [1 + \bar{g}^2 \ln(\omega_c/|\omega|)]}, \quad (17)$$

where D_{b}^R is given by Eq. (2). Depending on the temperature T , the quantum correction scales differently due to the competition between thermal and dynamical screening. The explicit expressions for the diagram amplitudes can be found in Ref. [73]. The quantum diagrams in Figs. 1(c)–(e) are analogous to those considered by Maekawa and Fukuyama [22, 25]. For readers unfamiliar with this notation, the analogous diagrams in conventional many-body perturbation theory are shown in

Fig. 1(f). For the case of repulsive Coulomb interactions, we recover the $\ln^3(\Lambda/T_c)$ suppression of T_c [22, 25, 27].

Upon summing up the diagrams, the total inverse pairing susceptibility in the static limit is found to be

$$[\chi_{\text{tot}}^R]^{-1}(0, \mathbf{0}) = -\frac{2N}{W} + \pi\nu_0 [N\mathcal{S}(t) + \mathcal{Q}(t)]. \quad (18)$$

The quantum correction

$$\mathcal{Q}(t) \simeq \begin{cases} \frac{\bar{g}^2 \mathcal{C}(t)}{\pi\nu_0 D t}, & t \gtrsim t_*, \\ 7.25 \sqrt{\frac{N \bar{g}^2}{2^3 \pi^4 \nu_0 D t}}, & t \ll t_*, \end{cases} \quad (19)$$

where $t = T/\gamma_{\text{el}}$ is the reduced temperature and $t_* \equiv 2\pi^2 \bar{g}^2 \nu_0 / (\alpha_m N)$. For $t \gtrsim t_*$, thermal screening dominates and the singularity in t originates from the thermal mass of the quantum-relaxational bosons [Eq. (2)]. For $t \ll t_*$, the thermal mass and dephasing drop out and the quantum correction diverges in a less singular manner. $\mathcal{C}(t)$ is a dimensionless parameter which varies weakly with T and depends on α , α_m , \bar{g}^2 and τ_{φ}^{-1} [73]. It encodes the integrals involved in Figs. 1(c)–(e).

The second and third terms in Eq. (18) correspond respectively to the semiclassical and quantum corrections. As the T -dependence of the semiclassical contribution $\mathcal{S}(T)$ is extremely weak, its primary effect is merely to enhance the BCS coupling W to W_{eff} :

$$W_{\text{eff}}^{-1} \equiv W^{-1} - (\pi\nu_0/2) \mathcal{S}(t_c). \quad (20)$$

Meanwhile, the quantum correction is singular in t owing to the quantum-critical nature of the bosons. Consequently, superconductivity is mainly driven by the quantum correction. As $T \rightarrow T_c$, $[\chi_{\text{tot}}^R]^{-1}(0, \mathbf{0}) \rightarrow 0$. Solving for T_c using Eq. (18) results in Eq. (1). The enhancement due to the quantum correction overcomes the MFL suppression and increases as \bar{g}^2 . This is the main result of this paper.

The physical origin of the enhancement is two-fold. On one hand, the quantum-critical interaction is magnified by the collective modes encoding the diffusive motion of the fermions. Physically, this is because the fermions have a higher probability to interact strongly with each other due to their slow diffusive motion [24, 26, 67]. This in turn amplifies the interaction in the BCS channel through operator mixing that results in multifractal enhancement [33, 37]. On the other hand, as the attractive $\text{SU}(N)$ Altshuler-Aronov conductance correction suppresses localization, fermions become more itinerant at low T [9, 70]. These two effects overcome the MFL suppression of the single-particle phase coherence and promote superconductivity through collective excitations. Our results differ from the suppressive Maekawa-Fukuyama quantum correction [22, 25, 27], owing to the attractive and long-ranged nature of the quantum-critical

interaction studied here.

Our work suggests a novel mechanism to boost superconductivity in a disordered quantum-critical system. Importantly, the robust superconductivity predicted by Eq. (1) demonstrates how collective phase coherence can survive in systems without well-defined quasiparticles. Similar conclusions apply to Altshuler-Aronov quantum corrections to the conductivity [9, 70, 79–81]. While the above calculation was carried out perturbatively in $1/\sigma_{\text{dc}}$, the physical picture is more general and we expect it to hold when higher-order corrections are included.

Conclusion.—We have demonstrated that the transition temperature T_c for superconductivity is boosted due to the interplay of attractive quantum-critical interactions and diffusive collective modes. Although the superconductivity is suppressed at the semiclassical level due to the extinction of well-defined quasiparticles, phase coherence is recovered at the quantum level through the collective modes. Our results are applicable to a broad range of quantum-critical materials where disorder is inevitable in practice. Remarkably, a recent experiment reported a significant increment of T_c in a cuprate superconductor by inducing disorder with proton irradiation [82], and in $\text{Y}_5\text{Rh}_6\text{Sn}_{18}$ by atomic disorder [83]. It would be interesting to further experimentally explore the effects of disorder on T_c in other strongly correlated quantum materials to test our predictions.

We thank Pavel Nosov and Sri Raghu for helpful discussions. This work was supported by the Welch Foundation Grant No. C-1809 (T.C.W. and M.S.F.) and by the DOE (US) office of Basic Sciences Grant No. DE-FG02-03ER46076 (P.L.).

-
- [1] C. M. Varma, P. B. Littlewood, S. S.-Rink, E. Abrahams, and A. E. Ruckenstein, Phenomenology of the normal state of Cu-O high-temperature superconductors, *Phys. Rev. Lett.* **63**, 1996 (1989).
- [2] B. Keimer, S. A. Kivelson, M. R. Norman, S. Uchida, and J. Zaanen, From quantum matter to high-temperature superconductivity in copper oxides, *Nature* **518**, 179 (2015).
- [3] Y. Cao, V. Fatemi, S. Fang *et al.*, Unconventional superconductivity in magic-angle graphene superlattices, *Nature* **556**, 43 (2018).
- [4] I. Esterlis, H. Guo, A. A. Patel, and S. Sachdev, Large- N theory of critical Fermi surfaces, *Phys. Rev. B* **103**, 235129 (2021).
- [5] E. E. Aldape, T. Cookmeyer, A. A. Patel, E. Altman, Solvable Theory of a Strange Metal at the Breakdown of a Heavy Fermi Liquid, *Phys. Rev. B* **105**, 235111 (2022).
- [6] H. Guo, A. A. Patel, I. Esterlis, S. Sachdev, Large N theory of critical Fermi surfaces II: conductivity, *Phys. Rev. B* **106**, 115151 (2022).
- [7] D. Chowdhury, A. Georges, O. Parcollet, and S. Sachdev, Sachdev-Ye-Kitaev Models and Beyond: A Window into Non-Fermi Liquids, *Rev. Mod. Phys.* **94**, 035004 (2022).
- [8] A. A. Patel, H. Guo, I. Esterlis, S. Sachdev, Universal T -linear resistivity in two-dimensional quantum-critical metals from spatially random interactions, arXiv:2203.04990 (2022).
- [9] T. C. Wu, Y. Liao, and M. S. Foster, Quantum Interference of Hydrodynamic Modes in a Dirty Marginal Fermi Liquid, *Phys. Rev. B* **106**, 155108 (2022).
- [10] S. Lederer, Y. Schattner, E. Berg, and S. A. Kivelson, Superconductivity and non-Fermi liquid behavior near a nematic quantum critical point, *Proc. Natl. Acad. Sci. U.S.A.* **114**, 19 (2017).
- [11] A. Abanov and A. V. Chubukov, Interplay between superconductivity and non-Fermi liquid at a quantum critical point in a metal. I. The γ model and its phase diagram at $T = 0$: The case $0 < \gamma < 1$, *Phys. Rev. B* **102**, 024524 (2020).
- [12] Y.-M. Wu, A. Abanov, Y. Wang, and A. V. Chubukov, Interplay between superconductivity and non-Fermi liquid at a quantum critical point in a metal. II. The γ model at a finite T for $0 < \gamma < 1$, *Phys. Rev. B* **102**, 024525 (2020).
- [13] Y.-M. Wu, A. Abanov, and A. V. Chubukov, Interplay between superconductivity and non-Fermi liquid behavior at a quantum critical point in a metal. III. The γ model and its phase diagram across $\gamma = 1$, *Phys. Rev. B* **102**, 094516 (2020).
- [14] Y.-M. Wu, S.-S. Zhang, A. Abanov, and A. V. Chubukov, Interplay between superconductivity and non-Fermi liquid at a quantum critical point in a metal. IV. The γ model and its phase diagram at $1 < \gamma < 2$, *Phys. Rev. B* **103**, 024522 (2021).
- [15] Y.-M. Wu, S.-S. Zhang, A. Abanov, and A. V. Chubukov, Interplay between superconductivity and non-Fermi liquid behavior at a quantum-critical point in a metal. V. The γ model and its phase diagram: The case $\gamma = 2$, *Phys. Rev. B* **103**, 184508 (2021).
- [16] S.-S. Zhang, Y.-M. Wu, A. Abanov, and A. V. Chubukov, Interplay between superconductivity and non-Fermi liquid at a quantum critical point in a metal. VI. The γ model and its phase diagram at $2 < \gamma < 3$, *Phys. Rev. B* **104**, 144509 (2021).
- [17] A. L. Chudnovskiy and A. Kamenev, Superconductor-Insulator Transition in a Non-Fermi Liquid, *Phys. Rev. Lett.* **129**, 266601 (2022).
- [18] C. Li, S. Sachdev, and D. G. Joshi, Superconductivity of non-Fermi liquids described by Sachdev-Ye-Kitaev models, arXiv:2208.05493 (2022).
- [19] P. A. Nosov, I. S. Burmistrov, and S. Raghu, Interplay of superconductivity and localization near a 2D ferromagnetic quantum critical point, *Phys. Rev. B* **107**, 144508 (2023).
- [20] P. W. Anderson, Theory of dirty superconductors, *J. Phys. Chem. Solids* **11**, 26 (1959).
- [21] A. A. Abrikosov, and L. P. Gorkov, On the Theory of Superconducting Alloys I. The Electrostatics of Alloys at Absolute Zero, *Sov. Phys. JETP* **8**, 1090 (1959).
- [22] S. Maekawa, and H. Fukuyama, Localization Effects in Two-Dimensional Superconductors, *J. Phys. Soc. Jpn.* **51**, 1380-1385 (1981).
- [23] M. Ma, and P. A. Lee, Localized superconductors, *Phys. Rev. B* **32**, 5658 (1985).
- [24] P. A. Lee and T. V. Ramakrishnan, Disordered electronic systems, *Rev. Mod. Phys.* **57**, 287 (1985).
- [25] A. M. Finkel'stein, Suppression of superconductivity in

- homogeneously disordered systems, *Physica B* **197**, 636 (1994).
- [26] D. Belitz and T. R. Kirkpatrick, The Anderson-Mott transition, *Rev. Mod. Phys.* **66**, 261 (1994).
- [27] M. V. Feigel'man, A. I. Larkin, and M. A. Skvortsov, Keldysh action for disordered superconductors, *Phys. Rev. B* **61**, 12361 (2000).
- [28] A. Ghosal, M. Randeria, and N. Trivedi, Role of Spatial Amplitude Fluctuations in Highly Disordered *s*-Wave Superconductors, *Phys. Rev. Lett.* **81**, 3940 (1998).
- [29] A. Ghosal, M. Randeria, and N. Trivedi, Inhomogeneous pairing in highly disordered *s*-wave superconductors, *Phys. Rev. B* **65**, 014501 (2001).
- [30] B. Fan and A. M. García-García, Superconductivity at the three-dimensional Anderson metal-insulator transition, *Phys. Rev. B* **102**, 184507 (2020).
- [31] M. V. Feigel'man, L. B. Ioffe, V. E. Kravtsov, and E. A. Yuzbashyan, Eigenfunction Fractality and Pseudogap State near the Superconductor-Insulator Transition, *Phys. Rev. Lett.* **98**, 027001 (2007).
- [32] M. V. Feigel'man, L. B. Ioffe, V. E. Kravtsov, E. Cuevas, Fractal superconductivity near localization threshold, *Annals of Physics*, **325**, 1390 (2010).
- [33] I.S. Burmistrov, I.V. Gornyi, A.D. Mirlin, Enhancement of the Critical Temperature of Superconductors by Anderson Localization, *Phys. Rev. Lett.* **108**(1), 017002 (2012).
- [34] M. S. Foster and E. A. Yuzbashyan, Interaction-Mediated Surface State Instability in Disordered Three-Dimensional Topological Superconductors with Spin SU(2) Symmetry, *Phys. Rev. Lett.* **109**, 246801 (2012).
- [35] M. S. Foster, H.-Y. Xie, and Y.-Z. Chou, Topological protection, disorder, and interactions: Survival at the surface of 3D topological superconductors, *Phys. Rev. B* **89**, 155140 (2014).
- [36] J. Mayoh, and A. M. García-García, Global critical temperature in disordered superconductors with weak multifractality, *Phys. Rev. B* **92**, 174526 (2015).
- [37] I. S. Burmistrov, I. V. Gornyi, and A. D. Mirlin, Superconductor-insulator transitions: Phase diagram and magnetoresistance, *Phys. Rev. B* **92**, 014506 (2015).
- [38] E. J. König, A. Levchenko, I. V. Protopopov, I. V. Gornyi, I. S. Burmistrov, and A. D. Mirlin, Berezinskii-Kosterlitz-Thouless transition in homogeneously disordered superconducting films, *Phys. Rev. B* **92**, 214503 (2015).
- [39] M. Stosiek, F. Evers, and I. S. Burmistrov, Multifractal correlations of the local density of states in dirty superconducting films, *Phys. Rev. Research* **3**, L042016 (2021).
- [40] I. S. Burmistrov, I. V. Gornyi, and A. D. Mirlin, Multifractally-enhanced superconductivity in thin films, *Ann. Phys.* **435**, 168499 (2021).
- [41] E. Arrighoni, E. Fradkin, and S. A. Kivelson, Mechanism of high-temperature superconductivity in a striped Hubbard model, *Phys. Rev. B* **69**, 214519 (2004).
- [42] I. Martin, D. Podolsky, and S. A. Kivelson, Enhancement of superconductivity by local inhomogeneities, *Phys. Rev. B* **72**, 060502(R) (2005).
- [43] K. Aryanpour, E. R. Dagotto, M. Mayr, T. Paiva, W. E. Pickett, and R. T. Scalettar, Effect of inhomogeneity on *s*-wave superconductivity in the attractive Hubbard model, *Phys. Rev. B* **73**, 104518 (2006).
- [44] K. Aryanpour, T. Paiva, W. E. Pickett, and R. T. Scalettar, *s*-wave superconductivity phase diagram in the inhomogeneous two-dimensional attractive Hubbard model, *Phys. Rev. B* **76**, 184521 (2007).
- [45] S. A. Kivelson and E. Fradkin, How Optimal Inhomogeneity Produces High Temperature Superconductivity, *Handbook of High-Temperature Superconductivity* edited by J. R. Schrieffer and J. S. Brooks (Springer, New York, 2007).
- [46] W.-F. Tsai, H. Yao, A. Läuchli, and S. A. Kivelson, Optimal inhomogeneity for superconductivity: Finite-size studies, *Phys. Rev. B* **77**, 214502 (2008).
- [47] F. Mondaini, T. Paiva, R. R. dos Santos, and R. T. Scalettar, Disordered two-dimensional superconductors: Roles of temperature and interaction strength, *Phys. Rev. B* **78**, 174519 (2008).
- [48] Y. Zou, I. Klich, and G. Refael, Effect of inhomogeneous coupling on BCS superconductors, *Phys. Rev. B* **77**, 144523 (2008).
- [49] M. Tezuka and A. M. García-García, Stability of the superfluid state in a disordered one-dimensional ultracold fermionic gas, *Phys. Rev. A* **82**, 043613 (2010).
- [50] V. Kravtsov, Wonderful life at weak Coulomb interaction: increasing of superconducting/superfluid transition temperature by disorder, *J. Phys.: Conf. Ser.* **376**, 012003 (2012).
- [51] R. Mondaini, T. Ying, T. Paiva, and R. T. Scalettar, Determinant quantum Monte Carlo study of the enhancement of *d*-wave pairing by charge inhomogeneity, *Phys. Rev. B* **86**, 184506 (2012).
- [52] Luca Dell'Anna, Enhancement of critical temperatures in disordered bipartite lattices, *Phys. Rev. B* **88**, 195139 (2013).
- [53] J. F. Dodaro and S. A. Kivelson, Generalization of Anderson's theorem for disordered superconductors, *Phys. Rev. B* **98**, 174503 (2018).
- [54] M. N. Gastiasoro and B. M. Andersen, Enhancing superconductivity by disorder, *Phys. Rev. B* **98**, 184510 (2018).
- [55] B. Sacépé, M. Feigel'man, T. M. Klapwijk, Quantum breakdown of superconductivity in low-dimensional materials, *Nat. Phys.* **16**, 734-746 (2020).
- [56] V. A. Zyuzin and A. M. Finkel'stein, Fluctuation-induced odd-frequency spin-triplet pairing in a disordered electron liquid, *Phys. Rev. B* **105**, 214523 (2022).
- [57] X. Zhang and M. S. Foster, Enhanced Amplitude for Superconductivity due to Spectrum-wide Wave Function Criticality in Quasiperiodic and Power-law Random Hopping Models, *Phys. Rev. B* **106**, L180503 (2022).
- [58] E. Abrahams, P. W. Anderson, P. A. Lee, and T. V. Ramakrishnan, Quasiparticle lifetime in disordered two-dimensional metals, *Phys. Rev. B* **24**, 6783 (1981).
- [59] S.-S. Lee, Recent Developments in Non-Fermi Liquid Theory, *Ann. Rev. of Cond. Matt. Phys.*, **9**, 227 - 244 (2018).
- [60] S. Sachdev, *Quantum Phase Transitions*, 2nd Ed., Cambridge University Press (2011).
- [61] E. Berg, S. Lederer, Y. Schattner, and S. Trebst, Monte Carlo Studies of Quantum Critical Metals, *Ann. Rev. of Cond. Matt. Phys.*, **10**, 63-84 (2019).
- [62] J. A. Damia, M. Solís, and G. Torroba, How non-Fermi liquids cure their infrared divergences, *Phys. Rev. B* **102**, 045147 (2020).
- [63] S. Raghu, G. Torroba, and H. Wang, Metallic quantum critical points with finite BCS couplings, *Phys. Rev. B* **92**, 205104 (2015).

- [64] I. S. Burmistrov, Finkel'stein Nonlinear Sigma Model: Interplay of Disorder and Interaction in 2D Electron Systems, *Journal of Experimental and Theoretical Physics* **129**, 669 (2019).
- [65] Y. Liao, A. Levchenko, and M. S. Foster, Response theory of the ergodic many-body delocalized phase: Keldysh Finkel'stein sigma models and the 10-fold way, *Ann. Phys.* **386**, 97 (2017).
- [66] A. M. Finkel'stein, Influence of Coulomb interaction on the properties of disordered metals, *Zh. Eksp. Teor. Fiz.* **84**, 168 (1983) [*Sov. Phys. JETP* **57**, 97 (1983)].
- [67] A. Kamenev, *Field Theory of Non-Equilibrium Systems*, 2nd ed. (Cambridge University Press, Cambridge, England, 2023).
- [68] A. Kamenev and A. Levchenko, Keldysh technique and non-linear σ -model: basic principles and applications, *Adv. Phys.* **58**, 197 (2009).
- [69] J. A. Damia, S. Kachru, S. Raghu, and G. Torroba, Two-Dimensional Non-Fermi-Liquid Metals: A Solvable Large- N Limit, *Phys. Rev. Lett.* **123**, 096402 (2019).
- [70] P. A. Nosov, I. S. Burmistrov, and S. Raghu, Interaction-Induced Metallicity in a Two-Dimensional Disordered Non-Fermi Liquid, *Phys. Rev. Lett.* **125**, 256604 (2020).
- [71] A. Altland and M. R. Zirnbauer, *Phys. Rev. B* **55**, 1142 (1997).
- [72] S. Ryu, A. P. Schnyder, A. Furusaki, and A. W. W. Ludwig, Topological insulators and superconductors: tenfold way and dimensional hierarchy, *New J. Phys.* **12**, 065010 (2010).
- [73] See the Supplemental Material for the precise definition of the sigma model and its parameterization, as well as the detailed calculation of the semiclassical and quantum terms in the pairing susceptibility, and which includes Ref. [74].
- [74] B. L. Altshuler and A. G. Aronov, Electron-electron interaction in disordered conductors, in *Electron-Electron Interactions in Disordered Systems*, edited by M. Pollak and A. L. Efros (North-Holland, Amsterdam, 1985).
- [75] H. Wang, S. Raghu, and G. Torroba, Non-Fermi-liquid superconductivity: Eliashberg approach versus renormalization group, *Phys. Rev. B* **95**, 165137 (2017).
- [76] L. Dell'Anna, Disordered d -wave superconductors with interactions, *Nucl. Phys. B* **758**, 255 (2006).
- [77] M. S. Foster and A. W. W. Ludwig, Metal-insulator transition from combined disorder and interaction effects in Hubbard-like electronic lattice models with random hopping, *Phys. Rev. B* **77**, 165108 (2008).
- [78] Y. Liao, M. S. Foster, Dephasing Catastrophe in $4 - \epsilon$ Dimensions: A Possible Instability of the Ergodic (Many-Body-Delocalized) Phase, *Phys. Rev. Lett.* **120**, 236601 (2018).
- [79] I. Paul, C. Pépin, B. N. Narozhny, and D. L. Maslov, Quantum Correction to Conductivity Close to a Ferromagnetic Quantum Critical Point in Two Dimensions, *Phys. Rev. Lett.* **95**, 017206 (2005).
- [80] V. M. Galitski, Metallic phase in a two-dimensional disordered Fermi system with singular interactions, *Phys. Rev. B* **72**, 214201 (2005).
- [81] T. Ludwig, I. V. Gornyi, A. D. Mirlin, and P. Wölfel, Effect of gauge-field interaction on fermion transport in two dimensions: Hartree conductivity correction and dephasing, *Phys. Rev. B* **77**, 235414 (2008).
- [82] M. Leroux, V. Mishra, J. P. C. Ruff, H. Claus, M. P. Smylie, C. Opagiste, P. Rodière, A. Kayani, G. D. Gu, J. M. Tranquada, W.-K. Kwok, Z. Islam, and U. Welp, Disorder raises the critical temperature of a cuprate superconductor, *Proc. Natl. Acad. Sci. U.S.A.*, **116**, 10691 (2019).
- [83] A. Ślebarski, M. Fijałkowski, P. Zajdel, M. M. Maška, J. Deniszczyk, M. Zubko, O. Pavlosiuk, K. Sasmal, and M. B. Maple, Enhancing superconductivity of $\text{Y}_5\text{Rh}_6\text{Sn}_{18}$ by atomic disorder, *Phys. Rev. B* **102**, 054514 (2020).

Enhancement of Superconductivity in a Dirty Marginal Fermi Liquid: Supplemental Material

Tsz Chun Wu,¹ Patrick A. Lee,² and Matthew S. Foster^{1,3}

¹*Department of Physics and Astronomy, Rice University, Houston, Texas 77005, USA*

²*Department of Physics, Massachusetts Institute of Technology, Cambridge, Massachusetts 02139, USA*

³*Rice Center for Quantum Materials, Rice University, Houston, Texas 77005, USA*

(Dated: May 24, 2023)

CONTENTS

| | | |
|-----|---|----|
| I. | The class AI non-linear sigma model | 1 |
| | A. Rotation of the saddle point and the $\pi - \sigma$ parameterization | 3 |
| | B. Feynman rules | 5 |
| II. | Pairing susceptibility | 6 |
| | A. Semiclassical contribution - The Cooper ladder | 6 |
| | B. Quantum interference correction | 7 |
| | 1. Thermal-screening dominated regime | 7 |
| | 2. Dynamical-screening dominated regime | 9 |
| | C. Overall pairing susceptibility | 9 |
| | 1. Without dynamical screening | 9 |
| | 2. With dynamical screening | 9 |
| | References | 10 |

I. THE CLASS AI NON-LINEAR SIGMA MODEL

We consider s -wave superconductivity with spin-singlet, flavor “triplet” pairing [Eq. (11) in the main text], in a system of disordered fermions with N flavors coupled to $SU(N)$ quantum-critical bosons [1–3]. In the presence of spin rotational and time-reversal symmetries, the system in the diffusive regime can be described by the class-AI Finkelstein non-linear sigma model (FNLsM), which is an effective field theory describing the diffusive collective modes of the fermions [3–8]. The derivation of the sigma model is similar to the one in class A. Upon disorder averaging and integrating out the fermions, followed by the gradient expansion we obtain the following partition function and action [3, 5],

$$Z = \int \mathcal{D}\hat{q} \mathcal{D}\hat{\phi} \mathcal{D}|\Delta|^2 e^{-S} \quad (1.1)$$

$$S = \frac{1}{8\lambda} \int_{\mathbf{x}} \text{Tr} [\nabla \hat{q} \cdot \nabla \hat{q}] + i \frac{\hbar}{2} \int_{\mathbf{x}} \text{Tr} \left\{ \hat{q} \left[\hat{\sigma}^3 (\hat{\omega} - \hat{\Sigma}) + i \eta \hat{\sigma}^3 \hat{\tau}^3 \right] \right\} \quad (1.2)$$

$$- \frac{i}{2} \int_{\Omega, \mathbf{k}} \text{Tr} \left\{ \hat{\phi}_{-\Omega, -\mathbf{k}}^{\text{T}} [\hat{D}_{\text{b}}(\Omega, \mathbf{k})]^{-1} \hat{\phi}_{\Omega, \mathbf{k}} \right\} - i \hbar \frac{g}{\sqrt{N}} \int_{\mathbf{x}} \text{Tr} \left[\left(\hat{\phi}^a \hat{\tau}^a \hat{E}_{11}^{\sigma} + \hat{s}^2 \hat{\phi}^{a\text{T}} \hat{\tau}^a \hat{s}^2 \hat{E}_{22}^{\sigma} \right) \hat{M}_F(\hat{\omega}) \hat{q}(\mathbf{x}) \hat{M}_F(\hat{\omega}) \right]$$

$$+ \frac{i\hbar}{2} \int_{\mathbf{x}} \text{Tr} \left[\left(\Delta^{\text{cl}} \hat{\sigma}^+ + \bar{\Delta}^{\text{cl}} \hat{\sigma}^- + \Delta^{\text{q}} \hat{\sigma}^+ \hat{\tau}^1 + \bar{\Delta}^{\text{q}} \hat{\sigma}^- \hat{\tau}^1 \right) \hat{M}_F(\hat{\omega}) \hat{q}(\mathbf{x}) \hat{M}_F(\hat{\omega}) \right] - i \frac{2N}{W} \int_{t, \mathbf{x}} \left(\bar{\Delta}^{\text{q}} \Delta^{\text{cl}} + \Delta^{\text{q}} \bar{\Delta}^{\text{cl}} \right).$$

The Pauli matrices $\hat{\tau}$, $\hat{\sigma}$, \hat{s} , and $\hat{\Theta}$ act respectively in the Keldysh, particle-hole, spin-1/2, and frequency spaces. $\hat{\Theta}^1$ is defined via $\langle \omega | \hat{\Theta}^1 | \omega' \rangle = 2\pi \delta(\omega + \omega')$, where ω is frequency. The thermal matrix \hat{M}_F is defined as

$$\hat{M}_F(\hat{\omega}) = \begin{bmatrix} 1 & F(\hat{\omega}) \\ 0 & -1 \end{bmatrix}_{\tau}, \quad (1.3)$$

where $F(\omega) = \tanh(\omega/2T)$ is the generalized Fermi distribution function and T denotes temperature. The subscript τ means that this is a matrix in the Keldysh space. For brevity, we work with the units $k_B = c = \hbar = 1$, where k_B is the Boltzmann constant, c is the speed of light, and \hbar is the Planck constant. The \hat{q} matrix $\hat{q} \rightarrow \hat{q}_{\sigma,\sigma';i,j;\omega_1,\omega_2;\alpha,\beta}^{a,b}(\mathbf{x})$ carries indices in $\{\sigma,\sigma'\} \in \{1,2\}$ particle-hole, $\{\alpha,\beta\} \in \{\uparrow,\downarrow\}$ spin-1/2, $\{i,j\} \in \{1,2,\dots,N\}$ flavor, and $\{a,b\} \in \{R,A\}$ Keldysh (fermion retarded/advanced [5]) spaces, as well as frequency labels $\{\omega_1,\omega_2\}$. It is subjected to the following constraints

$$\hat{q}^2 = 1, \quad \text{Tr}[\hat{q}] = 0, \quad \hat{s}^2 \hat{\sigma}^1 \hat{\tau}^1 \hat{\Theta}^1 \hat{q}^\top \hat{s}^2 \hat{\sigma}^1 \hat{\tau}^1 \hat{\Theta}^1 = \hat{q}. \quad (1.4)$$

In Eq. (1.2), we have employed the shorthand notations $\int_{t,\mathbf{x}} = \int dt \int d^2x$ and $\int_{\Omega,\mathbf{q}} = \int \frac{d\Omega}{2\pi} \int \frac{d^2q}{(2\pi)^2}$. We have also introduced the particle-hole-space projectors $\hat{E}_{11}^\sigma \equiv (1 + \hat{\sigma}^3)/2$, $\hat{E}_{22}^\sigma \equiv (1 - \hat{\sigma}^3)/2$, and $\hat{\sigma}^\pm \equiv (\hat{\sigma}^1 \pm i\hat{\sigma}^2)/2$. The coupling constants for the pure \hat{q} -matrix action are

$$h = \pi\nu_0, \quad \frac{1}{\lambda} = Dh, \quad (1.5)$$

where ν_0 is the density of states per channel, the diffusion constant is $D = v_F^2/(4\gamma_{\text{el}})$, and γ_{el} is the elastic impurity scattering rate. The small dimensionless parameter $\pi\lambda$ is the inverse conductance per channel.

In the above action S , we have Hubbard-Stratonovich (H.S.) decoupled the bare pairing interaction in the spin-singlet, flavor-“triplet” [Eq. (11)], s -wave channel, resulting in the H.S. fields $\Delta^{\text{cl},\mathbf{q}}$ and $\bar{\Delta}^{\text{cl},\mathbf{q}}$. W in the last term of Eq. (1.2) is the effective Bardeen-Cooper-Schrieffer (BCS) interaction strength.

The last term on the second line of Eq. (1.2) describes the linear coupling between the fermion-bilinear \hat{q} matrix and the matrix bosonic field $\hat{\phi} \rightarrow \phi_{ij}^a(\Omega, \mathbf{k})$, which carries Keldysh label $a = \text{cl}, \mathbf{q}$ and flavor indices $\{i,j\}$. This term mediates the S_{intI} interaction in Eq. (77) of Ref. [3]. The Keldysh matrices $\{\hat{\tau}^{\text{cl}}, \hat{\tau}^{\mathbf{q}}\} \equiv \{\hat{1}, \hat{\tau}^1\}$.

The $\text{SU}(N)$ boson propagator \hat{D}_{b} at the saddle-point level [3] is given by

$$\hat{D}_{\text{b}}(\Omega, \mathbf{k}) = \begin{bmatrix} D_{\text{b}}^K(\Omega, \mathbf{k}) & D_{\text{b}}^R(\Omega, \mathbf{k}) \\ D_{\text{b}}^A(\Omega, \mathbf{k}) & 0 \end{bmatrix}, \quad D_{\text{b}}^R(\Omega, \mathbf{k}) = -\frac{1}{2(\mathbf{k}^2 - i\alpha\Omega + \alpha_m T)}, \quad (1.6)$$

where α and α_m are constants. The $\alpha_m T$ term serves as the thermal mass for the quantum-critical bosons and generically arises due to symmetry-allowed quartic ϕ^4 interactions amongst the bosons [3, 9–11]. In contrast with the $|\omega|/k$ frequency structure in the clean case, the bosonic propagator now behaves diffusively due to disorder smearing. Such quantum-relaxational form of the bosonic propagator is quite generic and was also obtained in a slightly different model [9, 10].

The quantum-relaxational boson induces a marginal Fermi liquid (MFL) self-energy for the fermions [3, 9, 10, 12] (instead of $\sim |\omega|^{2/3}$), which enters the sigma model as the matrix

$$\hat{\Sigma}_{\hat{\omega}} = \begin{bmatrix} \hat{\Sigma}_{\text{MFL},\hat{\omega}}^R & 0 \\ 0 & \hat{\Sigma}_{\text{MFL},\hat{\omega}}^A \end{bmatrix}_\tau = \text{Re} \hat{\Sigma}_{\text{MFL},\hat{\omega}}^R + i \text{Im} \hat{\Sigma}_{\text{MFL},\hat{\omega}}^R \hat{\tau}^3, \quad \Sigma_{\text{MFL},\omega}^R = -\bar{g}^2 \left[\omega \ln \left(\frac{\omega_c}{x} \right) + i \frac{\pi}{2} x \right], \quad x = \max(|\omega|, JT). \quad (1.7)$$

Here J is a constant and $\bar{g}^2 = g^2/4\pi^2\gamma_{\text{el}}$ is the dimensionless squared Yukawa coupling constant. Note that the causality structure of the $\hat{\sigma}^3 \text{Im} \hat{\Sigma}_{\text{MFL},\hat{\omega}}$ term in the sigma model is consistent with the $i\eta \hat{\sigma}^3 \tau^3$ Keldysh prescription.

The S_{intII} term in Eq. (78) of Ref. [3] is a vertex-correction term that is crucial for the calculation of the density response function, in order to satisfy the Ward identity for charge conservation. It also prevents strange metallicity (linear- T resistivity) from manifesting *at the semiclassical level* for pure potential disorder [3, 9]. However S_{intII} is irrelevant for the discussion of the pairing susceptibility and we thus do not discuss this term further in this paper.

In the following, we present the parameterization of the FNLsM and the corresponding Feynman rules. Our main goal is to compute the pairing susceptibility and explore the consequences of the interplay between disorder and quantum-critical interactions on the superconducting transition temperature T_c . While we focus on a particular microscopic model here, the physics of the conclusion is quite general and expected to be applicable to a wide range of disordered quantum-critical systems.

A. Rotation of the saddle point and the $\pi - \sigma$ parameterization

To facilitate the parameterization, we perform a unitary rotation [5]

$$\hat{q} \rightarrow \hat{R} \hat{q} \hat{R}, \quad \hat{R} = \hat{E}_{11}^\sigma + \hat{E}_{22}^\sigma \hat{\tau}^1, \quad (1.8)$$

where $\hat{E}_{11,22}^\sigma$ are defined above Eq. (1.5), so that the saddle point becomes

$$\hat{q}_{\text{sp}} \rightarrow \hat{\tau}_3. \quad (1.9)$$

The symmetry constraints for \hat{q} are now

$$\hat{q}^2 = 1, \quad \text{Tr}[\hat{q}] = 0, \quad \hat{s}^2 \hat{\sigma}^1 \hat{\Theta}^1 \hat{q}^\top \hat{s}^2 \hat{\sigma}^1 \hat{\Theta}^1 = \hat{q}. \quad (1.10)$$

We then employ the “ π - σ ” parameterization for the \hat{q} matrix

$$\hat{q} = \begin{bmatrix} \sqrt{1 - \hat{W}^\dagger \hat{W}} & \hat{W}^\dagger \\ \hat{W} & -\sqrt{1 - \hat{W} \hat{W}^\dagger} \end{bmatrix}_\tau = \hat{q}^{(0)} + \hat{q}^{(1)} + \hat{q}^{(2)} + \hat{q}^{(4)} + \dots \quad (1.11)$$

where

$$\hat{q}^{(0)} = \hat{\tau}^3, \quad (1.12)$$

$$\hat{q}^{(1)} = \begin{bmatrix} 0 & \hat{W}^\dagger \\ \hat{W} & 0 \end{bmatrix}_\tau, \quad (1.13)$$

$$\hat{q}^{(2)} = \frac{1}{2} \begin{bmatrix} -\hat{W}^\dagger \hat{W} & 0 \\ 0 & \hat{W} \hat{W}^\dagger \end{bmatrix}_\tau, \quad (1.14)$$

$$\hat{q}^{(4)} = \frac{1}{8} \begin{bmatrix} -(\hat{W}^\dagger \hat{W})^2 & 0 \\ 0 & (\hat{W} \hat{W}^\dagger)^2 \end{bmatrix}_\tau, \quad (1.15)$$

and the \hat{W} field satisfies

$$\hat{W} = \hat{s}^2 \hat{\sigma}^1 \hat{\Theta}^1 (\hat{W}^\dagger)^\top \hat{s}^2 \hat{\sigma}^1 \hat{\Theta}^1, \quad (1.16)$$

which follows immediately from Eq. (1.10).

We further introduce the unconstrained, \mathbb{C} -valued matrix fields \hat{X} and \hat{Y} defined by

$$X_{ij;\omega_1,\omega_2;\alpha\beta}(\mathbf{k}) = W_{ij;\omega_1,\omega_2;\alpha\beta}^{+,+}(\mathbf{k}), \quad Y_{ij;\omega_1,\omega_2;\alpha\beta}(\mathbf{k}) = W_{ij;\omega_1,\omega_2;\alpha\beta}^{+,-}(\mathbf{k}). \quad (1.17)$$

To satisfy the constraint in Eq. (1.16), we can write

$$\hat{W} = \begin{bmatrix} \hat{X} & \hat{Y} \\ \hat{\Theta}^1 \hat{s}^2 (\hat{Y}^\dagger)^\top \hat{\Theta}^1 \hat{s}^2 & \hat{\Theta}^1 \hat{s}^2 (\hat{X}^\dagger)^\top \hat{\Theta}^1 \hat{s}^2 \end{bmatrix}_\sigma. \quad (1.18)$$

We then plug Eqs. (1.11) and (1.18) back into the FNLsM and expand the action in Eq. (1.2) up to quartic order.

To facilitate the perturbative expansion in λ , which is proportional to inverse conductance, we rescale $\hat{X} \rightarrow \sqrt{\lambda} \hat{X}$, $\hat{Y} \rightarrow \sqrt{\lambda} \hat{Y}$ [3, 5]. At quadratic order, the action is given by

$$S_X^{(2)} = \frac{1}{2} \int \text{Tr} \left[\hat{X}_{1,2}^\dagger(\mathbf{k}_1) M_{2,1;4,3}(\mathbf{k}_1, \mathbf{k}_2) \hat{X}_{3,4}(\mathbf{k}_2) + I_{2,1}^\dagger(\mathbf{k}) \hat{X}_{1,2}(\mathbf{k}) + I_{2,1}(\mathbf{k}) \hat{X}_{1,2}^\dagger(\mathbf{k}) \right], \quad (1.19)$$

$$S_Y^{(2)} = \frac{1}{2} \int \text{Tr} \left[\hat{Y}_{1,2}^\dagger(\mathbf{k}_1) N_{2,1;4,3}(\mathbf{k}_1, \mathbf{k}_2) \hat{Y}_{3,4}(\mathbf{k}_2) + J_{2,1}^\dagger(\mathbf{k}) \hat{Y}_{1,2}(\mathbf{k}) + J_{2,1}(\mathbf{k}) \hat{Y}_{1,2}^\dagger(\mathbf{k}) \right], \quad (1.20)$$

where the numerical subscripts $\{1, 2, 3, 4\}$ correspond to frequencies $\{\omega_1, \omega_2, \omega_3, \omega_4\}$, $f = \int_{1,2,3,4,\mathbf{k}}$ integrates over all

frequencies and momentum, and Tr traces over the flavor and spin-1/2 labels. We also defined

$$\begin{aligned} M_{2,1;4,3}(\mathbf{k}_1, \mathbf{k}_2) &= [\Delta_{2,1}^X(\mathbf{k}_1)]^{-1} \delta_{1,4} \delta_{2,3} \delta_{\mathbf{k}_1, \mathbf{k}_2} \\ &+ ih\lambda \frac{1}{\sqrt{N}} [\hat{\phi}_{4-1}^{\text{cl}}(\mathbf{k}_1 - \mathbf{k}_2) + F_4 \hat{\phi}_{4-1}^{\text{q}}(\mathbf{k}_1 - \mathbf{k}_2)] \delta_{2,3} \\ &+ ih\lambda \frac{1}{\sqrt{N}} [-\hat{\phi}_{2-3}^{\text{cl}}(\mathbf{k}_1 - \mathbf{k}_2) + F_3 \hat{\phi}_{2-3}^{\text{q}}(\mathbf{k}_1 - \mathbf{k}_2)] \delta_{1,4}, \end{aligned} \quad (1.21)$$

$$\begin{aligned} N_{2,1;4,3}(\mathbf{k}_1, \mathbf{k}_2) &= [\Delta_{2,1}^Y(\mathbf{k}_1)]^{-1} \delta_{1,4} \delta_{2,3} \delta_{\mathbf{k}_1, \mathbf{k}_2} \\ &+ ih\lambda \frac{1}{\sqrt{N}} [\hat{\phi}_{4-1}^{\text{cl}}(\mathbf{k}_1 - \mathbf{k}_2) - F_1 \hat{\phi}_{4-1}^{\text{q}}(\mathbf{k}_1 - \mathbf{k}_2)] \delta_{2,3} \\ &+ ih\lambda \frac{1}{\sqrt{N}} [-\hat{\phi}_{2-3}^{\text{cl}}(\mathbf{k}_1 - \mathbf{k}_2) + F_3 \hat{\phi}_{2-3}^{\text{q}}(\mathbf{k}_1 - \mathbf{k}_2)] \delta_{1,4}, \end{aligned} \quad (1.22)$$

$$I_{2,1}^\dagger(\mathbf{k}) = 2ih\sqrt{\lambda} \frac{1}{\sqrt{N}} [(F_2 - F_1) \hat{\phi}_{2-1}^{\text{cl}}(-\mathbf{k}) + (1 - F_1 F_2) \hat{\phi}_{2-1}^{\text{q}}(-\mathbf{k})], \quad (1.23)$$

$$I_{2,1}(\mathbf{k}) = 2ih\sqrt{\lambda} \frac{1}{\sqrt{N}} \hat{\phi}_{2-1}^{\text{q}}(\mathbf{k}), \quad (1.24)$$

$$J_{2,1}^\dagger(\mathbf{k}) = 2ih\sqrt{\lambda} \frac{1}{\sqrt{N}} (\bar{\Delta}_{1-2}^{\text{cl}}(\mathbf{k}) - F_1 \bar{\Delta}_{1-2}^{\text{q}}(\mathbf{k})), \quad (1.25)$$

$$J_{2,1}(\mathbf{k}) = 2ih\sqrt{\lambda} \frac{1}{\sqrt{N}} (\Delta_{2-1}^{\text{cl}}(\mathbf{k}) - F_1 \Delta_{2-1}^{\text{q}}(\mathbf{k})), \quad (1.26)$$

where the Dirac delta functions $\delta_{\omega_1, \omega_2} \equiv \delta_{1,2} \equiv 2\pi \delta(\omega_1 - \omega_2)$ and $\delta_{\mathbf{k}_1, \mathbf{k}_2} = (2\pi)^2 \delta^{(2)}(\mathbf{k}_1 - \mathbf{k}_2)$.

The bare propagators are given by

$$\left\langle X_{i,j;1,2;\alpha,\beta}(\mathbf{k}) X_{k,l;3,4;\delta,\gamma}^\dagger(\mathbf{k}) \right\rangle_0 = 2\Delta_{1,2}^X(\mathbf{k}) \delta_{1,4} \delta_{2,3} \delta_{il} \delta_{jk} \delta_{\alpha\gamma} \delta_{\beta,\delta}, \quad (1.27)$$

$$\left\langle Y_{i,j;1,2;\alpha,\beta}(\mathbf{k}) Y_{k,l;3,4;\delta,\gamma}^\dagger(\mathbf{k}) \right\rangle_0 = 2\Delta_{1,2}^Y(\mathbf{k}) \delta_{1,4} \delta_{2,3} \delta_{il} \delta_{jk} \delta_{\alpha\gamma} \delta_{\beta,\delta}, \quad (1.28)$$

$$\Delta_{1,2}^X(\mathbf{k}) = \frac{1}{k^2 + ih\lambda(\omega_1 - \omega_2) + ih\lambda\bar{g}^2(\omega_1 \ln \frac{\omega_c}{x_1} - \omega_2 \ln \frac{\omega_c}{x_2}) + h\lambda \tau_{\text{MFL}}^{-1}}, \quad (1.29)$$

$$\Delta_{1,2}^Y(\mathbf{k}) = \frac{1}{k^2 + ih\lambda(\omega_1 + \omega_2) + ih\lambda\bar{g}^2(\omega_1 \ln \frac{\omega_c}{x_1} + \omega_2 \ln \frac{\omega_c}{x_2}) + h\lambda \tau_{\text{MFL}}^{-1}}, \quad (1.30)$$

where $x_{1,2} = \max(|\omega_{1,2}|, JT)$ and $\tau_{\text{MFL}}^{-1} = \bar{g}^2 \pi JT$ is the dephasing rate due to the MFL self-energy $\hat{\Sigma}_{\text{MFL}}$ [Eq. (1.7)]. Note: the prefactor 2 in Eqs. (1.27) and (1.28) is due to the prefactor 1/2 in the Gaussian action.

At quartic order, there are five Hikami box terms [5]. The relevant one responsible for the pairing susceptibility to the leading order of λ is

$$S_q^{(4)} = \frac{\lambda}{4} \int \delta_{\mathbf{k}_1 + \mathbf{k}_3, \mathbf{k}_2 + \mathbf{k}_4} \square_{1,2,3,4}^{\mathbf{k}_1, \mathbf{k}_2, \mathbf{k}_3, \mathbf{k}_4} \text{Tr} \left[\hat{X}_{1,2}(\mathbf{k}_1) \hat{s}^2 \hat{Y}_{3,-2}^\dagger(-\mathbf{k}_2) \hat{X}_{4,3}^\dagger(-\mathbf{k}_3) \hat{s}^2 Y_{-4,1}^\dagger(\mathbf{k}_4) \right], \quad (1.31)$$

where Tr traces over the flavor and spin indices, T is the transpose in the flavor \otimes spin space, and

$$\square_{1,2,3,4}^{\mathbf{k}_1, \mathbf{k}_2, \mathbf{k}_3, \mathbf{k}_4} = \begin{bmatrix} -(\mathbf{k}_1 \cdot \mathbf{k}_3 + \mathbf{k}_2 \cdot \mathbf{k}_4) + \frac{1}{2}(\mathbf{k}_1 + \mathbf{k}_3) \cdot (\mathbf{k}_2 + \mathbf{k}_4) \\ + i \frac{h}{2} \lambda (\omega_1 - \omega_2 + \omega_3 - \omega_4 - \Sigma_{\text{MFL},1}^R + \Sigma_{\text{MFL},2}^A - \Sigma_{\text{MFL},3}^R + \Sigma_{\text{MFL},4}^A) \end{bmatrix}. \quad (1.32)$$

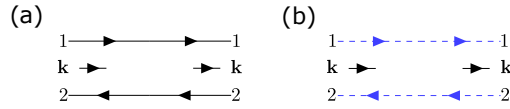


FIG. I.1. The diagrammatic representation of the propagators for (a) diffusons (\hat{X} fields) and (b) Cooperons (\hat{Y} fields). The arrows on these lines represent frequency flow in the propagators. The numerical labels 1, 2 are shorthand notations for frequencies ω_1, ω_2 . Meanwhile, the short arrows between the two lines indicate the momentum (\mathbf{k}) flow.

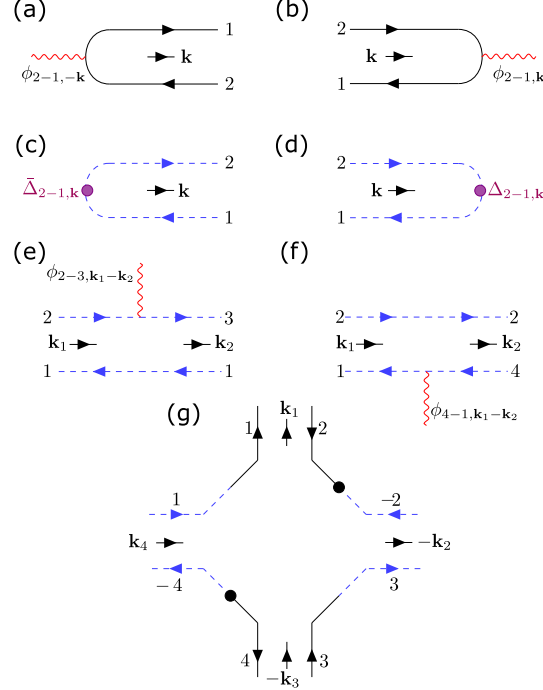


FIG. I.2. The feynman diagrams representing the vertices relevant for evaluating the pairing susceptibility [see Eqs. (1.33)–(1.38)]. The diffuson (Cooperon) propagator is represented diagrammatically by two black solid (blue dashed) lines with arrows pointing in the opposite directions (see Fig. I.1). The red wavy line denotes the bosonic field ϕ . The vertex for converting between the Hubbard-Stratonovich Cooper pairing field $\Delta^{c/q}$ and the Cooperon mode is denoted by the purple dot.

B. Feynman rules

We adopt the same convention for the Feynman rules presented in Refs. [3, 5]. The diffuson (Cooperon) propagator is represented diagrammatically in Figs. I.1 (a) [(b)] by two black solid lines (blue dashed lines) with arrows pointing in the opposite directions. The frequency indices of the matrix fields \hat{X} (\hat{Y}) and \hat{X}^\dagger (\hat{Y}^\dagger) are labeled by the numbers. The flavor and spin indices are implicit. Along a solid line, the frequency label, spin, and flavor indices remain unchanged. The momentum flowing through the diffuson is labeled by an arrow in the middle of the two black solid lines. The momentum arrow points inwards (outwards) for the fields \hat{X}, \hat{Y} ($\hat{X}^\dagger, \hat{Y}^\dagger$).

The interaction vertices are diagrammatically depicted in Fig. I.2. The corresponding amplitudes are given by

$$\text{Fig. I.2(a)} = -ih\sqrt{\lambda}[(F_2 - F_1)\phi_{2-1,-\mathbf{k}}^{\text{cl}} + (1 - F_1F_2)\phi_{2-1,-\mathbf{k}}^{\text{q}}]/\sqrt{N}, \quad (1.33)$$

$$\text{Fig. I.2(b)} = -ih\sqrt{\lambda}\phi_{2-1,\mathbf{k}}^{\text{q}}/\sqrt{N}, \quad (1.34)$$

$$\text{Fig. I.2(c)} = -ih\sqrt{\lambda}[\bar{\Delta}_{1-2,\mathbf{k}}^{\text{cl}} - F_1\bar{\Delta}_{1-2,\mathbf{k}}^{\text{q}}], \quad (1.35)$$

$$\text{Fig. I.2(d)} = -ih\sqrt{\lambda}[\Delta_{2-1,\mathbf{k}}^{\text{cl}} - F_1\Delta_{2-1,\mathbf{k}}^{\text{q}}], \quad (1.36)$$

$$\text{Fig. I.2(e)} = -\frac{ih}{2}\lambda[-\phi_{2-3,\mathbf{k}_1-\mathbf{k}_2}^{\text{cl}} + F_3\phi_{2-3,\mathbf{k}_1-\mathbf{k}_2}^{\text{q}}]/\sqrt{N}, \quad (1.37)$$

$$\text{Fig. I.2(f)} = -\frac{ih}{2}\lambda[\phi_{4-1,\mathbf{k}_1-\mathbf{k}_2}^{\text{cl}} - F_1\phi_{4-1,\mathbf{k}_1-\mathbf{k}_2}^{\text{q}}]/\sqrt{N}, \quad (1.38)$$

$$\text{Fig. I.2(g)} = -\frac{\lambda}{4}\square_{1,2,3,4}^{\mathbf{k}_1,\mathbf{k}_2,\mathbf{k}_3,\mathbf{k}_4}. \quad (1.39)$$

II. PAIRING SUSCEPTIBILITY

A. Semiclassical contribution - The Cooper ladder

The retarded inverse pairing susceptibility $[\chi_{\text{semi}}^R]^{-1}$ can be obtained by computing the effective propagator of Δ^{cl} and $\bar{\Delta}^{\text{q}}$. At the semiclassical level (ignoring quantum interference), we only consider the linear coupling between \hat{Y}, \hat{Y}^\dagger and $\Delta, \bar{\Delta}$. By integrating out the \hat{Y} fields, we have

$$i[\chi_{\text{semi}}^R]^{-1}(\omega, \mathbf{k}) = -i\frac{2N}{W} + 4h^2\lambda N \int_{\varepsilon} \frac{F_{\varepsilon - \frac{\omega}{2}}}{k^2 - 2ih\lambda\varepsilon + ih\lambda\bar{g}^2 \left[(-\varepsilon + \omega/2) \ln \frac{\omega_c}{|-\varepsilon + \omega/2|} - (\varepsilon + \omega/2) \ln \frac{\omega_c}{|\varepsilon + \omega/2|} \right] + h\lambda\tau_\varphi^{-1}}, \quad (2.1)$$

where τ_φ^{-1} is the effective dephasing rate incorporating τ_{MFL}^{-1} and the Cooperon self-energies represented by the diagrams in Fig. 18 of Ref. [5]. The corresponding Feynman diagram for the second term in Eq. (2.1) is depicted in Fig. II.1(a), which is equivalent to summing the Cooper ladders [13]. In the static limit $\omega = 0$ and $k \rightarrow 0$, we have

$$i[\chi_{\text{semi}}^R]^{-1}(0, \mathbf{0}) = -i\frac{2N}{W} + 4hN \int_{\varepsilon} \frac{F_{\varepsilon}}{-2i\varepsilon\mathcal{A}_{\text{MFL}}(\varepsilon) + \tau_\varphi^{-1}}, \quad (2.2)$$

where the marginal Fermi liquid (MFL) self-energy [Eq. (1.7)] is encoded by the factor

$$\mathcal{A}_{\text{MFL}}(\varepsilon) = 1 + \bar{g}^2 \ln \frac{\omega_c}{\max(JT, |\varepsilon|)} > 1. \quad (2.3)$$

In the absence of the MFL effects, $\bar{g}^2 \rightarrow 0$, and the above expression reduces to the FL result [4, 14]. At the proximity of the transition temperature $T \rightarrow T_c$, $[\chi_{\text{semi}}^R]^{-1} \rightarrow 0$. If we assume $\tau_\varphi^{-1} \ll T_c$ for simplicity, then

$$0 = [\chi_{\text{semi}}^R]^{-1}(0, \mathbf{0}) = -\frac{2N}{W} + \frac{2hN}{\pi} \int_0^{\Lambda/2T_c} dy \frac{\tanh(y)}{y\mathcal{A}_{\text{MFL}}(2T_c y)} \quad (2.4)$$

$$\simeq -\frac{2N}{W} + \frac{2hN}{\pi} \frac{1}{\bar{g}^2} \ln \left(1 + \bar{g}^2 \ln \frac{\Lambda}{T_c} \right), \quad (2.5)$$

implying that

$$T_c \simeq \Lambda \exp \left[-\frac{1}{\bar{g}^2} \left(e^{\pi\bar{g}^2/hW} - 1 \right) \right], \quad (2.6)$$

which is much smaller than the BCS result. Physically, the strong suppression of the transition temperature is due to the MFL self-energy that destroys well-defined quasiparticles before they can form Cooper pairs.

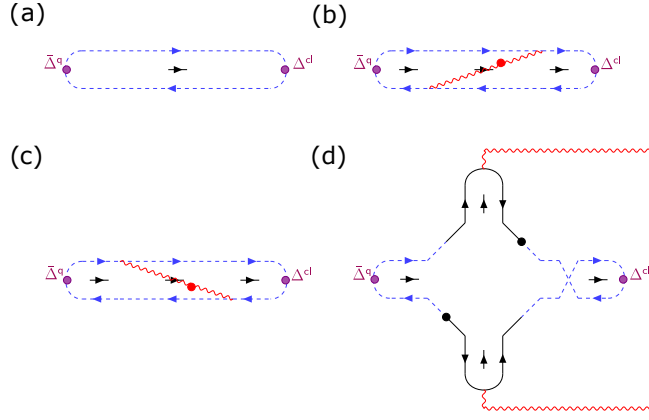


FIG. II.1. The Feynman diagrams responsible for the pairing susceptibility (the same as Fig. 1 in the main text). (a): the semiclassical contribution, and (b)–(d): the quantum interference corrections to the leading order in λ , which is proportional to the inverse conductance.

B. Quantum interference correction

Despite the absence of well-defined quasiparticles, phase coherence can still manifest through collective modes. In the following, we consider the quantum correction to the pairing susceptibility represented by the diagrams in Figs. II.1(b)–(d). The corresponding expressions are respectively given by

$$\text{Fig. II.1(b)} = 4h^4 \lambda^3 g^2 \int_{\varepsilon_1, \varepsilon_2, \mathbf{q}} \Delta_{\varepsilon_1, \varepsilon_1}^Y(\mathbf{k}) \Delta_{\varepsilon_2, \varepsilon_2}^Y(\mathbf{k}) \Delta_{\varepsilon_1, \varepsilon_2}^Y(\mathbf{k} + \mathbf{q}) (-F_{\varepsilon_1^+}) i \left[F_{\varepsilon_2^-} D_{\mathbf{b}, \varepsilon_1 - \varepsilon_2}^A(\mathbf{q}) + F_{\varepsilon_1^-} D_{\mathbf{b}, \varepsilon_1 - \varepsilon_2}^R(\mathbf{q}) \right], \quad (2.7)$$

$$\text{Fig. II.1(c)} = 4h^4 \lambda^3 g^2 \int_{\varepsilon_1, \varepsilon_2, \mathbf{q}} \Delta_{\varepsilon_1, \varepsilon_1}^Y(\mathbf{k}) \Delta_{\varepsilon_2, \varepsilon_2}^Y(\mathbf{k}) \Delta_{\varepsilon_1, \varepsilon_2}^Y(\mathbf{k} + \mathbf{q}) (-F_{\varepsilon_1^+}) i \left[F_{\varepsilon_1^-} D_{\mathbf{b}, \varepsilon_1 - \varepsilon_2}^R(\mathbf{q}) + F_{\varepsilon_2^+} D_{\mathbf{b}, \varepsilon_1 - \varepsilon_2}^A(\mathbf{q}) \right], \quad (2.8)$$

$$\text{Fig. II.1(d)} = 8h^4 \lambda^3 g^2 \int_{\varepsilon_1, \varepsilon_2, \mathbf{q}} \Delta_{\varepsilon_1, \varepsilon_1}^Y(\mathbf{k}) \Delta_{\varepsilon_2, \varepsilon_2}^Y(\mathbf{k}) [\Delta_{\varepsilon_1, -\varepsilon_2}^X(\mathbf{q})]^2 \square_{\varepsilon_1^+, -\varepsilon_2^+, \varepsilon_2^-, -\varepsilon_1^-}^{\mathbf{q}, -\mathbf{k}, -\mathbf{q}, \mathbf{k}} F_{\varepsilon_1^+} (-F_{\varepsilon_1} - F_{\varepsilon_2}) i D_{\mathbf{b}, \varepsilon_1 + \varepsilon_2}^R(\mathbf{q}), \quad (2.9)$$

where $\varepsilon^\pm = \varepsilon \pm \omega/2$. Due to the Cooperon self-energy, τ_{MFL}^{-1} in the propagator Δ^Y should be replaced by the total dephasing rate $\tau_\varphi^{-1} = \tau_{\text{MFL}}^{-1} + \tau_C^{-1}$. In the above expressions, we omitted terms proportional to the Keldysh component of bosonic propagator; these can be absorbed into the dephasing rate [5].

1. Thermal-screening dominated regime

For $T \gtrsim T_*$, thermal screening is more important than dynamical screening and thus the bosonic propagator can be approximated by the quantum relaxational version $D_{\mathbf{b}}$ [Eq. (2) in the main text]. Here the thermal-to-dynamical screening crossover temperature is defined via

$$T^* \equiv \frac{g^2 \nu_0}{2\alpha_m N}, \quad (2.10)$$

where $\alpha_m = m_b^2/T$ is the coefficient of the quantum-relaxational boson thermal mass.

In the thermal screening regime, by focusing on the static limit $\omega \rightarrow 0$, $k \rightarrow 0$ and performing the q integral, we have

$$\text{Fig. II.1(b)} + \text{Fig. II.1(c)} + \text{Fig. II.1(d)} \simeq -i h \lambda \mathcal{C} \frac{\bar{g}^2}{t}, \quad (2.11)$$

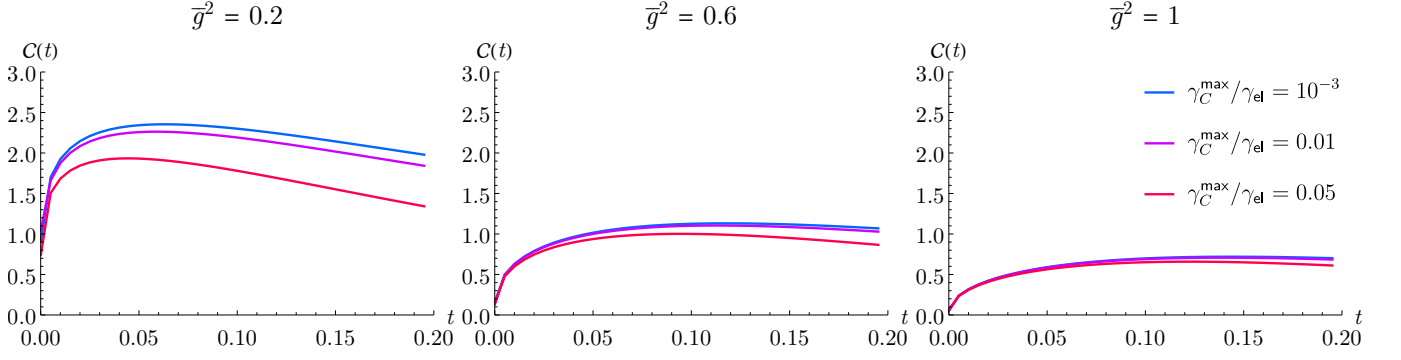


FIG. II.2. Plot of $\mathcal{C}(t)$ as a function of the reduced temperature $t = T/\gamma_{\text{el}}$ in the thermal-screening dominated regime, based on Eq. (2.12). Here, the parameters are $h = 1$, $\lambda = 0.02$, $\alpha_m = \alpha = 0.5$, $J = 1$, $\Lambda = \gamma_{\text{el}} = 10$ and $\gamma_C = \tau_C^{-1}$ is the dephasing rate. We phenomenologically take a linear- T dephasing rate $\gamma_C(t) = \gamma_C^{\text{max}}(t/t_{\text{max}})$, where $t_{\text{max}} = 0.2$.

where $t = T/\gamma_{\text{el}}$, and the dimensionless parameter

$$\mathcal{C}(t) = -\frac{h}{\pi} \int dy_1 dy_2 \frac{\tanh y_1}{[2iy_1 \mathcal{A}_{\text{MFL}}(2Ty_1) + \frac{1}{2T\tau_\varphi}][2iy_2 \mathcal{A}_{\text{MFL}}(2Ty_2) + \frac{1}{2T\tau_\varphi}]} \times \left[\begin{array}{l} \Phi(y_1, y_2, \alpha, \alpha_m, \tau_\varphi^{-1}, \lambda) \tanh y_1 \\ + \Phi(y_1, y_2, -\alpha, \alpha_m, \tau_\varphi^{-1}, \lambda) \tanh y_2 \\ + \Phi_H(y_1, y_2, \alpha, \alpha_m, \tau_{\text{MFL}}^{-1}, \lambda)(\tanh y_1 + \tanh y_2) \end{array} \right], \quad (2.12)$$

with

$$\begin{aligned} \Phi(y_1, y_2, \alpha, \alpha_m, \tau_\varphi^{-1}, \lambda, \bar{g}^2, T) &\equiv -2T \int_0^\infty dx \Delta_{2Ty_1, 2Ty_2}^Y(x) D_{\text{b}, 2T(y_1 - y_2)}^R(x) \\ &= \frac{1}{-ih\lambda[2y_1 \mathcal{A}_{\text{MFL}}(2Ty_1) + 2y_2 \mathcal{A}_{\text{MFL}}(2Ty_2)] - h\lambda \frac{\tau_\varphi^{-1}}{T} + \alpha_m - 2i\alpha(y_1 - y_2)} \\ &\times \ln \left\{ \frac{\alpha_m - 2i\alpha(y_1 - y_2)}{ih\lambda[2y_1 \mathcal{A}_{\text{MFL}}(2Ty_1) + 2y_2 \mathcal{A}_{\text{MFL}}(2Ty_2)] + h\lambda \frac{\tau_\varphi^{-1}}{T}} \right\}, \end{aligned} \quad (2.13)$$

and similarly

$$\begin{aligned} \Phi_H(y_1, y_2, \alpha, \alpha_m, \tau_{\text{MFL}}^{-1}, \lambda, \bar{g}^2, T) &\equiv -2T \int_0^\infty dx \Delta_{2Ty_1, -2Ty_2}^X(x) D_{\text{b}, 2T(y_1 + y_2)}^R(x) \\ &= \frac{1}{-ih\lambda[2y_1 \mathcal{A}_{\text{MFL}}(2Ty_1) + 2y_2 \mathcal{A}_{\text{MFL}}(2Ty_2)] - h\lambda \frac{\tau_{\text{MFL}}^{-1}}{T} + \alpha_m - 2i\alpha(y_1 + y_2)} \\ &\times \ln \left\{ \frac{\alpha_m - 2i\alpha(y_1 + y_2)}{ih\lambda[2y_1 \mathcal{A}_{\text{MFL}}(2Ty_1) + 2y_2 \mathcal{A}_{\text{MFL}}(2Ty_2)] + h\lambda \frac{\tau_{\text{MFL}}^{-1}}{T}} \right\}. \end{aligned} \quad (2.14)$$

Note that since the MFL and total dephasing rates, τ_{MFL}^{-1} and τ_φ^{-1} respectively, are proportional to temperature, \mathcal{C} is just a function of $\ln T$ and thus only weakly depends on temperature. We plot $\mathcal{C}(t)$ versus the dimensionless temperature $t = T/\gamma_{\text{el}}$ in Fig. II.2 for various model parameters.

2. Dynamical-screening dominated regime

We now consider the regime $T \ll T_*$ in which dynamical screening dominates over thermal screening. Repeating the above calculation using the dynamically screened bosonic propagator D_{scr} [see Eq. (16) in the main text], we obtain a new version of Φ . The full expression is very complicated, but for small T ,

$$\Phi_{\text{scr}}(y_1, y_2) = \frac{\pi\sqrt{T}}{2\sqrt{2i}(y_2 - y_1)\beta} + \mathcal{O}(T) \quad (2.15)$$

where $\beta = 2h^2g^2\lambda/\pi N$. This contribution arises from the regime where $q^2 \sim 2Ty_{1,2}$, where q is the loop momentum in Eqs. (2.7)–(2.9). The dimensionless parameter \mathcal{C} then becomes

$$\mathcal{C}_{\text{scr}} \simeq -\frac{h}{\pi} \int dy_1 dy_2 \frac{\tanh y_1}{(2iy_1)(2iy_2)} \left[\begin{aligned} &(\Phi_{\text{scr}}(y_1, y_2) \tanh y_1 + \Phi_{\text{scr}}^*(y_1, y_2) \tanh y_2) \\ &+ \Phi_{\text{scr}}(y_1, -y_2)(\tanh y_1 + \tanh y_2). \end{aligned} \right] \quad (2.16)$$

By numerically evaluating the remaining integral, we have

$$\text{Re } \mathcal{C}_{\text{scr}} \simeq 7.25 \frac{h}{\pi} \sqrt{\frac{T}{\beta}} = 7.25 \frac{h}{\pi} \sqrt{\frac{T}{2h^2g^2\lambda/\pi N}} = 7.25 \sqrt{\frac{NT}{2\pi g^2\lambda}} = 7.25 \sqrt{\frac{Nt}{(2\pi)^3 \bar{g}^2 \lambda}}. \quad (2.17)$$

C. Overall pairing susceptibility

1. Without dynamical screening

Combining both the semiclassical and quantum contributions, the total inverse pairing susceptibility at the transition temperature $t \rightarrow t_c$ is

$$[\chi^R]^{-1}(0, \mathbf{0}) = -\frac{2N}{W} + \frac{hN}{\pi} \frac{1}{\bar{g}^2} \ln \left(1 + \bar{g}^2 \ln \frac{1}{t_c} \right) + \frac{\lambda h \bar{g}^2 \mathcal{C}}{t_c}. \quad (2.18)$$

Since the second term has a weak temperature dependence, it just effectively renormalizes the pairing interaction strength W , Eq. (20) in the main text. By combining the first two terms as $-2N/W_{\text{eff}}$, we have

$$t_c \simeq \frac{\lambda h \bar{g}^2 \mathcal{C}}{2N} W_{\text{eff}}, \quad (2.19)$$

valid up to some logarithmic corrections. Since $\pi\lambda$ is the inverse conductance per channel, the full conductivity accounting for 2 spin and N flavor components is

$$\sigma_{\text{dc}} = \frac{2N}{\pi\lambda}. \quad (2.20)$$

With $h = \pi\nu_0$, $T_c = t_c \gamma_{\text{el}}$ and $\gamma_{\text{el}} \bar{g}^2 = g^2/4\pi^2$, we recover Eq. (1) in the main text for $T \gg T^*$.

2. With dynamical screening

For $T \ll T_*$, dynamical screening becomes important and the inverse pairing susceptibility is instead

$$\begin{aligned} [\chi^R]^{-1}(0, \mathbf{0}) &= -\frac{2N}{W} + \frac{hN}{\pi} \frac{1}{\bar{g}^2} \ln \left(1 + \bar{g}^2 \ln \frac{1}{t_c} \right) + \frac{\lambda h \bar{g}^2}{t_c} 7.25 \sqrt{\frac{Nt_c}{(2\pi)^3 \bar{g}^2 \lambda}} \\ &= -\frac{2N}{W} + \frac{hN}{\pi} \frac{1}{\bar{g}^2} \ln \left(1 + \bar{g}^2 \ln \frac{1}{t_c} \right) + 7.25 h \sqrt{\frac{N\lambda \bar{g}^2}{(2\pi)^3 t_c}}. \end{aligned} \quad (2.21)$$

Thus, we have (by combining the first two terms as $-2N/W_{\text{eff}}$)

$$t_c = \frac{\lambda\bar{g}^2}{(2\pi)^3 N \left(\frac{2}{7.25 h W_{\text{eff}}}\right)^2} = \frac{\lambda\bar{g}^2 (h W_{\text{eff}})^2}{(2\pi)^3 N \left(\frac{2}{7.25}\right)^2} \simeq 0.05 \frac{\lambda\bar{g}^2 (h W_{\text{eff}})^2}{N}. \quad (2.22)$$

This is Eq. (1) in the main text for $T \ll T^*$.

-
- [1] J. A. Damia, S. Kachru, S. Raghu, and G. Torroba, Two-Dimensional Non-Fermi-Liquid Metals: A Solvable Large- N Limit, *Phys. Rev. Lett.* **123**, 096402 (2019).
 - [2] P. A. Nosov, I. S. Burmistrov, and S. Raghu, Interaction-Induced Metallicity in a Two-Dimensional Disordered Non-Fermi Liquid, *Phys. Rev. Lett.* **125**, 256604 (2020).
 - [3] T. C. Wu, Y. Liao, and M. S. Foster, Quantum Interference of Hydrodynamic Modes in a Dirty Marginal Fermi Liquid, *Phys. Rev. B* **106**, 155108 (2022).
 - [4] A. Kamenev and A. Levchenko, Keldysh technique and non-linear σ -model: basic principles and applications, *Adv. Phys.* **58**, 197 (2009).
 - [5] Y. Liao, A. Levchenko, and M. S. Foster, Response theory of the ergodic many-body delocalized phase: Keldysh Finkel'stein sigma models and the 10-fold way, *Ann. Phys.* **386**, 97 (2017).
 - [6] A. M. Finkel'stein, Influence of Coulomb interaction on the properties of disordered metals, *Zh. Eksp. Teor. Fiz.* **84**, 168 (1983) [*Sov. Phys. JETP* **57**, 97 (1983)].
 - [7] D. Belitz and T. R. Kirkpatrick, The Anderson-Mott transition, *Rev. Mod. Phys.* **66**, 261 (1994).
 - [8] I. S. Burmistrov, Finkel'stein Nonlinear Sigma Model: Interplay of Disorder and Interaction in 2D Electron Systems, *Journal of Experimental and Theoretical Physics* **129**, 669 (2019).
 - [9] A. A. Patel, H. Guo, I. Esterlis, and S. Sachdev, Universal theory of strange metals from spatially random interactions, *arXiv:2203.04990* (2022).
 - [10] H. Guo, Aavishkar A. Patel, I. Esterlis, and S. Sachdev, Large N theory of critical Fermi surfaces II: conductivity, *Phys. Rev. B* **106**, 115151 (2022).
 - [11] J. A. Damia, M. Solís, and G. Torroba, How non-Fermi liquids cure their infrared divergences, *Phys. Rev. B* **102**, 045147 (2020).
 - [12] C. M. Varma, P. B. Littlewood, S. S.-Rink, E. Abrahams, and A. E. Ruckenstein, Phenomenology of the normal state of Cu-O high-temperature superconductors, *Phys. Rev. Lett.* **63**, 1996 (1989).
 - [13] B. L. Altshuler and A. G. Aronov, Electron-electron interaction in disordered conductors, in *Electron-Electron Interactions in Disordered Systems*, edited by M. Pollak and A. L. Efros (North-Holland, Amsterdam, 1985).
 - [14] A. Kamenev, *Field Theory of Non-Equilibrium Systems*, 2nd ed. (Cambridge University Press, Cambridge, England, 2023).